Inorganic Chemistry

Article

pubs.acs.org/IC

Synthesis and Characterization of ^{68}Ga-Labeled Curcumin and Curcuminoid Complexes as Potential Radiotracers for Imaging of Cancer and Alzheimer's Disease

Mattia Asti,*[,†] Erika Ferrari,[‡] Stefania Croci,[§] Giulia Atti,[†] Sara Rubagotti,[†] Michele Iori,[†] Pier C. Capponi,[†] Alessandro Zerbini,[§] Monica Saladini,[‡] and Annibale Versari[†]

[†]Nuclear Medicine Unit, Oncology and Advanced Technologies Department, IRCCS-Arcispedale Santa Maria Nuova, Reggio Emilia, Italy

[‡]Department of Chemical and Geological Sciences, University of Modena, via Campi, 183, 41125 Modena, Italy

[§]Clinical Immunology, Allergy, and Advanced Biotechnologies Unit, Diagnostic Imaging and Laboratory Medicine Department, IRCCS-Arcispedale Santa Maria Nuova, Reggio Emilia, Italy

Supporting Information

ABSTRACT: Curcumin (CUR) and curcuminoids complexes labeled with fluorine-18 or technetium-99m have recently shown their potential as diagnostic tools for Alzheimer's disease. Gallium-68 is a positron-emitting, generator-produced radionuclide, and its properties can be exploited in situ in medical facilities without a cyclotron. Moreover, CUR showed a higher uptake in tumor cells compared to normal cells, suggesting potential diagnostic applications in this field. In spite of this, no studies using labeled CUR have been performed in this direction, so far. Herein, ^{68}Ga-labeled complexes with CUR and two curcuminoids, namely diacetyl-curcumin (DAC) and bis(dehydroxy)curcumin (bDHC), were synthesized and characterized by means of experimental and theoretical approaches. Moreover, a first evaluation of their affinity to synthetic β-amyloid fibrils and uptake by A549 lung cancer cells was performed to show the potential application of these new labeled curcuminoids in these diagnostic fields. The radiotracers were prepared by reacting $^{68}Ga^{3+}$ obtained from a $^{68}Ge/^{68}Ga$ generator with 1 mg/mL curcuminoids solutions. Reaction parameters (precursor amount, reaction temperature, and pH) were optimized to obtain high and reproducible radiochemical yield and purity. Stoichiometry and formation of the curcuminoid complexes were investigated by matrix-assisted laser desorption ionization time-of-flight mass spectrometry, NMR, ultraviolet−visible, and fluorescence spectroscopy on the equivalent ^{nat}Ga-curcuminoids (nat = natural) complexes, and their structure was computed by theoretical density functional theory calculations. The analyses evidenced that CUR, DAC, and bDHC were predominantly in the keto−enol form and attested to $Ga(L)_2^+$ species formation. Identity of the $^{68}Ga(L)_2^+$ complexes was confirmed by coelution with the equivalent $^{nat}Ga(L)_2^+$ complexes in ultrahigh-performance liquid chromatography analyses. $^{68}Ga(CUR)_2^+$, $^{68}Ga(DAC)_2^+$, and $^{68}Ga(bDHC)_2^+$ were highly (87 ± 4, 90 ± 1%) and moderately (48 ± 2%), respectively, retained by synthetic β-amyloid fibrils in vitro. All the Ga-curcuminoid complexes showed an uptake in A549 lung cancer cells, at least equivalent to the respective free curcuminoids, confirming potential applications as cancer-detecting radiotracers.

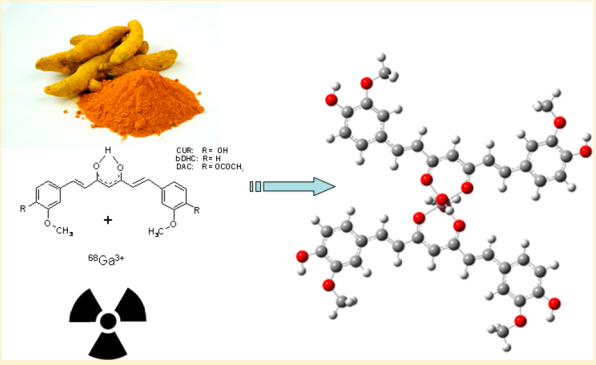

1. INTRODUCTION

Recently, curcumin (CUR) and curcuminoid complexes with metals have been subjected to a large number of studies due to their interesting potential as therapeutics in varying diseases. For example, iron and copper complexes of CUR seem to have high potential in the treatment of cancer,[1] while gallium complexes have remarkable antiviral effects on HSV-1 in cell culture.[2] Curcumin is a phyto-compound and dietary spice extracted from the rhizome of the herb *Curcuma longa* L., commonly known as turmeric. It is commonly used in traditional medicines of eastern world countries thanks to its properties such as antioxidant, anti-inflammatory, antimicrobial, and anticancer activities. In spite of its potential in therapeutic applications, the bioavailability of CUR is limited because of its low solubility and stability in aqueous media. This issue may be overcome in three ways, mainly: (i) by modifying the structure of CUR itself to increase its chemical stability and solubility but also to preserve its beneficial properties; (ii) by focusing the investigation on the properties of CUR/curcuminoid complexes that often exhibit higher solubility in aqueous media than free ligands; and (iii) by carrying CUR or CUR derivatives in

Received: December 20, 2013
Published: April 25, 2014

   dx.doi.org/10.1021/ic403113z | *Inorg. Chem.* 2014, 53, 4922−4933

drug delivery systems like liposomal or polymeric nanoparticles.[3] Curcumin structure includes a heptadiene with two 3-methoxy, 4-hydroxy phenyl groups, and an α,β-diketone. The α,β-diketone group is subjected to a pH and solvent-dependent keto−enol tautomerism that also influences the CUR metal-chelation capability.[4] The keto−enolic moiety of CUR has also been exploited in the complexation of radioactive metals for synthesizing ^{99m}Tc-labeled radiopharmaceuticals, where CUR acts as an OO bidentate ligand on a ^{99m}Tc-tricarbonyl core, with the aim of projecting probes to improve the diagnosis of Alzheimer's disease (AD) or cancer.[5] Although technectium-99m is the most commonly used radionuclide for nuclear medicine applications, in the most recent years, notable attention has been focused on innovative biomolecules labeled with gallium-68 since it is a generator-produced radionuclide, such as technetium-99m; but gallium-68 is also a positron emitter with suitable energy and half-life (89% β^+, maximum energy = 1.92 MeV, $T_{1/2}$ = 67.7 min) useful for many applications in nuclear medicine.[6] On the other hand, the features and the coordination properties of trivalent gallium are well-known from its traditional "cold" chemistry and can be exploited for developing new radiotracers. Recently, we synthesized and characterized some CUR derivatives with modifications on the aromatic rings, namely, diacetyl-curcumin (DAC) and bis(dehydroxy)curcumin (bDHC), that show both enhanced chemical stability and high cytotoxicity against different tumor cells lines.[7] The aim of the present study is to investigate the feasibility of the labeling of CUR and its derivatives, shown in Figure 1, with gallium-68 to obtain

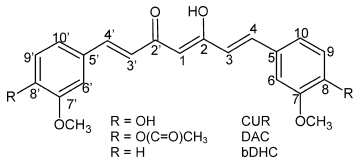

Figure 1. Chemical structure of investigated curcuminoids.

potential diagnostic tools for cancer and Alzheimer's disease. For this purpose, a complete characterization of the equivalent ^{nat}Ga (nat = natural) complexes structure and properties was performed by means of experimental and theoretical approaches.

2. RESULTS AND DISCUSSION

2.1. Characterization of ^{nat}Ga-Curcuminoid Complexes by Mass Spectrometry. Mass spectrometry represents a powerful and informative technique, which has been widely applied to curcuminoids and its metabolites.[8] Nevertheless, its utilization for the analysis of CUR-based metal complexes[9] has been limited so far, mainly due to the fact that CUR complexes have only in the last years achieved great interest in medical applications.[10] Recently, collision-induced dissociation tandem mass spectrometry (CID-MS/MS) with electrospray ionization (ESI) was applied to compare the stabilities of monodemethoxycurcumin-metal complexes with those of CUR ones. Herein, matrix-assisted laser desorption ionization mass spectrometry (MALDI-MS) was employed to investigate the stoichiometry of Ga-curcuminoid complexes at various metal-to-ligand molar ratios (M/L = 1:1, 1:2, 1:5, and 1:10). The comparison between the experimental data and the calculated values confirmed the formation of only the 1:2 molar ratio species in spite of the metal-to-ligand molar ratios used for the experiments. As an example, the mass spectra obtained for the 1:2 M/L system are reported in Figure 2. Analogous results were observed for large excesses of ligand with respect to the metal (1:10) as well as for equimolar ratio. Simulated isotopic spectral pattern also confirmed the formation of GaL_2^+ species for all analyzed curcuminoids.

2.2. Theoretical DFT Calculations. As previously reported,[4] CUR derivatives undergo keto−enol tautomerism, which is strongly affected by solvent polarity/proticity and electronic effects of the substituents both on the aromatic rings and on the central carbon atom of the diketo group. For instance, the absence of a bulky moiety in the α position of the carbonyls shifts the equilibrium almost completely toward the keto−enolic form, as confirmed for CUR by theoretical calculations, spectroscopic, and NMR data.[11] Moreover, CUR strongly stabilizes the keto−enolic form by three intramolecular hydrogen bonds: the first one between enolic proton and carbonyl oxygen, and the latter two between the phenolic hydrogen and methoxyl oxygen on aromatic rings, respectively.

Theoretical density functional theory (DFT) calculations were herein performed on free curcuminoids (CUR, DAC, and bDHC) and their gallium complexes $[GaL_2(H_2O)_2]^+$ to assess the effect of the substituents on the aromatic rings on the stabilization of gallium(III) complexes. Because of the acetyl groups in the para position of the aromatic rings, optimization by theoretical DFT calculations of DAC is extremely time-consuming; thus, the crystal structure reported by Mague et al.[12] was chosen as a starting point to optimize the geometry of DAC and its monoanion. Figure 3 shows the most stable optimized structures for bDHC and DAC, while those of CUR were previously reported by the authors.[11] The most stable conformers were selected as representative to construct the corresponding gallium complex structures. An octahedral coordination environment for gallium was achieved by adding two water molecules to the $Ga(L)_2^+$ complexes (Figure 4), as previously suggested by Xu et al.[13] In Table 1 the total energy values (E) for all ligands and their corresponding monoanion species originated from the dissociation of the enolic proton, as well as their $Ga(L)_2^+$ complexes, are reported. Binding energy (BE) values were calculated for metal complexes according to eq 1:

$$BE = TE_S - TE_C \quad \text{(eq 1)}$$

where TE_S is the sum of the total electronic energy of the bare metal ion and the relative isomer of the complexing anion, and TE_C represents the total electronic energy of metal complexes. The predicted geometry of Ga^{3+} complexes was similar for all ligands, even if BE values showed a slight thermodynamic stabilization of $[Ga(bDHC)_2(H_2O)_2]^+$ with respect to $[Ga(CUR)_2(H_2O)_2]^+$ and $[Ga(DAC)_2(H_2O)_2]^+$. This data hints at a destabilizing effect that is chiefly due to the steric hindrance of the substituents on the aromatic ring of the curcuminoids (in the order $-OCOCH_3 \gg -OH > -H$).

2.3. Nuclear Magnetic Resonance. The ^{1}H and ^{13}C NMR chemical shifts of free ligands and their complexes (Ga^{3+}/L = 1:2) are reported in Table 2. These data are useful for understanding the coordinating mode of the ligands and for providing insight into the complexes' structures. NMR data confirmed the formation of Ga^{3+} complexes, which are in slow chemical exchange with the free ligands in the NMR time scale. Actually, the addition of Ga^{3+} to the ligand solution induced the appearance of a new set of signals with the same spectral pattern of the free ligands but shifted to lower field, hinting at

dx.doi.org/10.1021/ic403113z | Inorg. Chem. 2014, 53, 4922−4933

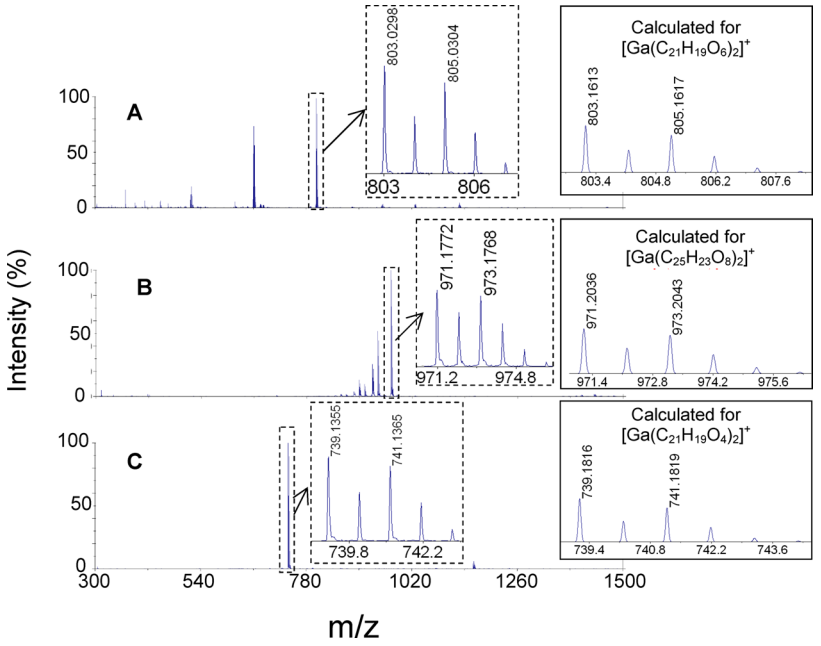

Figure 2. MALDI-TOF-MS mass spectra of $^{nat}Ga^{3+}$/curcuminoid 1:2 systems for CUR (A), DAC (B), and bDHC (C). Broken-line expansion highlights the typical isotopic spectral pattern of the experimentally observed gallium complexes $Ga(L)_2^+$ in comparison with the corresponding calculated ones (solid-line expansion).

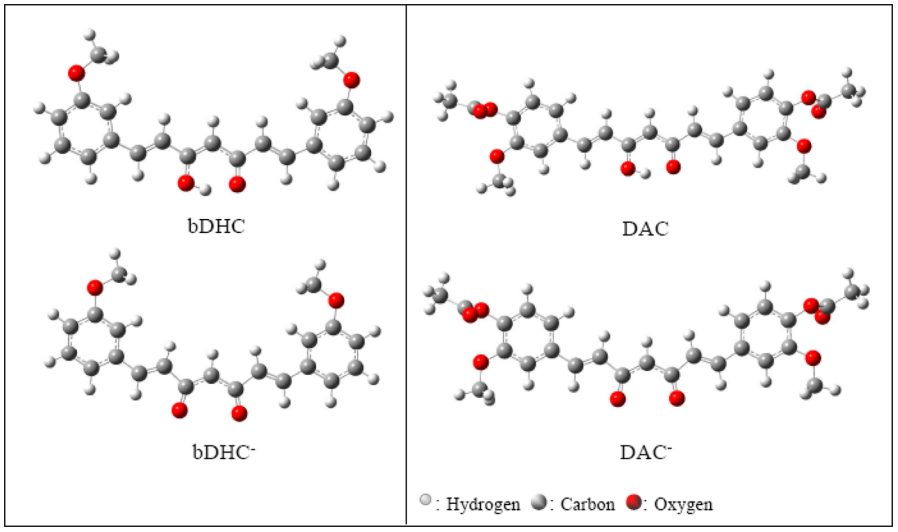

Figure 3. The final optimized structures of the most stable conformer and its monoanion at B3LYP/6-31G* level for bDHC and DAC.

the formation of a coordination compound. Strong shifts were observed for ^1H and ^{13}C signals of the aliphatic chain, especially for H-3, H-4, and C-1, C-2, C-3, and C-4. No significant shifts were instead observed for aromatic protons and carbons consistent with the OO donor set due to the keto−enol structure. All ligands showed similar behavior and, as an example, the ^1H NMR spectra of free CUR and Ga-CUR at 1:2 metal-to-ligand molar ratio in CD_3OD are reported in Figure 5, while ^1H NMR spectra of bDHC, DAC, and related M/L complexes at a 1:2 molar ratio are given as Supporting Information (Figure 1S).

^{71}Ga NMR studies were also performed to shed light on the coordination geometry of the investigated systems. Unfortunately, due to very fast quadrupolar relaxation of the ^{71}Ga nucleus, none of the complexes gave observable resonances. This outcome may suggest an unsymmetrical coordination environment of a relatively large complex, as reported in literature.[14,15]

Although two-dimensional (2D) nuclear Overhauser enhancement spectroscopy (NOESY) experiments were performed on $Ga(CUR)_2^+$ in MeOD-d_4, they were quite ineffective in giving structural information on gallium complexes. This was probably due to the high symmetry and pseudoplanarity of the CUR-like backbone and to the low number of protons, which are quite distant in the complexes structure. On the other hand, one-dimensional (1D) selective NOE experiments provided some information on the orientation of the aromatic rings that differed from that which was computed in the *ab inito* DFT calculations. These differences are probably due to the presence of a solvation sphere (methanol) that was not simulated in the DFT calculation. In particular, the selective irradiation on H-4 provides a NOE effect on $-OCHH_3$, suggesting its spatial

dx.doi.org/10.1021/ic403113z | Inorg. Chem. 2014, 53, 4922−4933

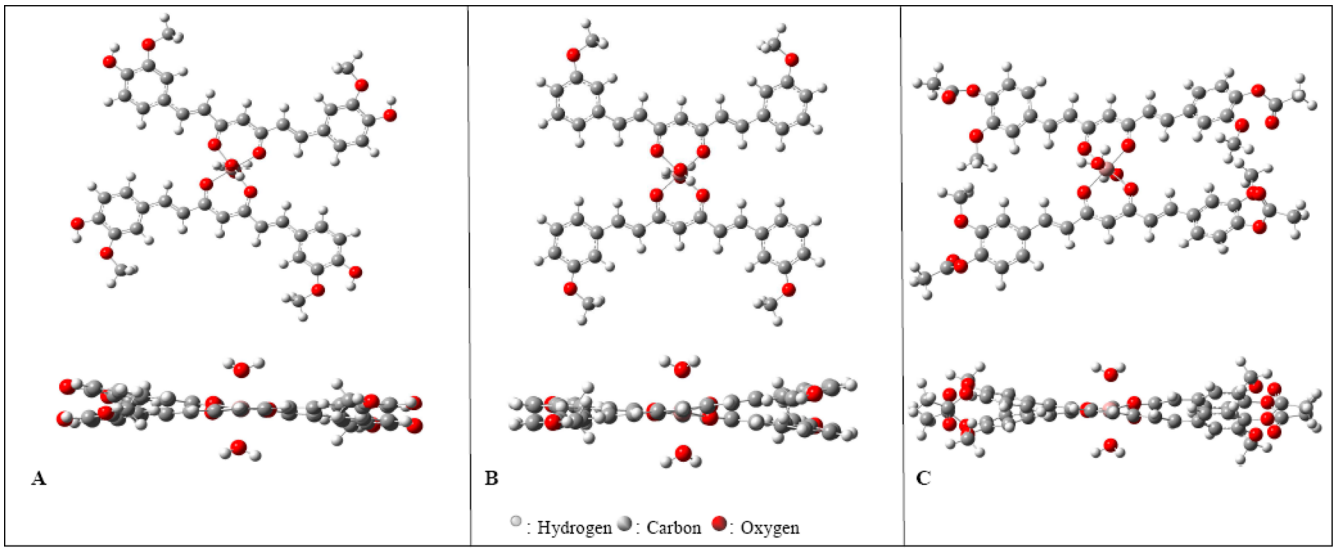

Figure 4. The final optimized structures of Ga^{3+} complexes at B3LYP/6-31G* level for CUR (A), bDHC (B), and DAC (C).

Table 1. B3LYP/6-31G* Total Energy *E* (a.u.) and Binding Energy BE (kcal/mol) for CUR, bDHC, DAC, Their Anionic Species, and Ga^{3+} Complexes

	E	BE
HCUR	−1263.573 277	
CUR^-	−1262.998 524	
HbDHC	−1113.134 602	
$bDHC^-$	−1112.564 545	
HDAC	−1568.882 446	
DAC^-	−1568.314 294	
$[Ga(CUR)_2(H_2O)_2]^+$	−4601.730 957	1346.77
$[Ga(bDHC)_2(H_2O)_2]^+$	−4300.845 589	1355.84
$[Ga(DAC)_2(H_2O)_2]^+$	−5212.342 859	1322.09

proximity (Supporting Information, Figure 2S). Unfortunately, due to the chemical shift equivalence, it is not possible to predict if the NOE effect is due to the spatial correlation between two spin systems (i.e., H-4 and OCH_3) in the same molecule or in two different molecules linked to the same Ga^{3+} ion.

2.4. UV−vis and Fluorescence Spectroscopy. Curcumin is a fluorescent molecule emitting in the visible spectrum (450−650 nm), and its emission is strongly dependent on solvent polarity and proticity, which regulate the equilibrium between the two tautomeric forms: keto−enol and diketo. However, due to extended conjugation and intramolecular hydrogen bonding, the predominant form is usually the keto−enol, resulting in a main absorbance peak at 420 nm, while only a weak shoulder due to diketo absorption centered around 350 nm was observed.[4] Consequently, CUR and its analogues may be employed as fluorescent markers, allowing distribution studies in cells and tissues.[16] With the aim of investigating the effect of complexation on emission spectra, ultraviolet−visible (UV−vis) and fluorescence spectroscopies in varying solvents (namely, water, phosphate-buffered saline (PBS) solution (pH = 7.4), and MeOH) were applied to Ga^{3+}/curcuminoid systems. Moreover, since serum albumins are well-established carriers for a large number of hydrophobic ligands,[17] bovine serum albumin (BSA) was chosen to investigate the fluorescence behavior of free curcuminoids and their Ga^{3+} complexes, with the purpose of simulating the cellular environment. In the conditions chosen for the experiments, the value of absorbance at λ_{max} for the free ligands and their gallium complexes in solution was lower than 0.2, making them suitable for the acquisition of excitation spectra.

The formation of Ga^{3+}/CUR complexes in MeOH was investigated at 298 K by fluorescence spectroscopy to confirm the 1:2 molar ratio determined by using mass spectrometry and to derive the effect of complexation on emission spectra. The spectra were obtained at λ_{ex} = 420 nm, corresponding to λ_{max} of the CUR absorption spectrum. As shown in Figure 6, fluorescence emission was increasingly quenched by the metal addition up to a 1:2 molar ratio. Conversely, bDHC and DAC showed a different behavior, since they were mildly fluorescent in MeOH (λ_{ex} = 400 nm), and the addition of Ga^{3+} ion slightly increased the fluorescence emission (Supporting Information, Figure 3S).

In aqueous solution, free curcuminoids exhibited broad absorption (Supporting Information, Figure 4S), and the maxima were determined at 424, 385, and 395 nm for CUR, DAC, and bDHC, respectively. These results clearly indicate that, similarly to CUR, DAC and bDHC were predominantly in the keto−enol form. A similar spectral pattern was observed for the corresponding Ga^{3+} complexes with maxima at 412, 388, and 417 nm for $[Ga(CUR)_2]^+$, $[Ga(DAC)_2]^+$, and $[Ga(bDHC)_2]^+$, respectively, and with absorption shoulders around 472, 450, and 449 nm for $[Ga(CUR)_2]^+$, $[Ga(DAC)_2]^+$, and $[Ga(bDHC)_2]^+$, respectively, showing a slight blue-shift for $[Ga(CUR)_2]^+$ and a red-shift for $[Ga(DAC)_2]^+$ and $[Ga(bDHC)_2]^+$.

Molar extinction coefficients (ε) of free curcuminoids and their Ga^{3+} metal complexes at λ = 400, 420, and 488 nm are reported in Table 3. Some considerations may be inferred: (i) for each species, ε increases according to solvent system in the order PBS (pH 7.4) < H_2O (pH 5) < BSA (5 mg/mL; pH 7.4), suggesting a stabilizing effect due to the interaction of both free ligands and gallium complexes with BSA; (ii) although $[GaL_2]^+$ = 1:2[L], the ratio between the value of ε of GaL_2^+ complexes and their free ligands in aqueous systems is always greater than 2. This finding confirms the formation of a new species, namely the gallium complex, with a higher molar extinction coefficient with respect to the ligand; (iii) in the presence of BSA at 400

dx.doi.org/10.1021/ic403113z | Inorg. Chem. 2014, 53, 4922−4933

Table 2. ^{1}H and ^{13}C Chemical Shifts (δ) of Free Ligands and GaL_2^+ in MeOD-d_4 at 298 K

	δ^a	1	2	3	4	5	6	7	8	9	10	CH_3O-	CH_3COO-
CUR	^{1}H	5.99		6.65	7.60		7.24			6.84	7.13	3.94	
		s, 1H		d, 2H	d, 2H		d, 2H			d, 2H	dd, 2H		
				$^{3}J_{3-4}$ 15.8 Hz	$^{3}J_{3-4}$ 15.8 Hz		$^{4}J_{6-10}$ 1.8 Hz			$^{3}J_{9-10}$ 8.3 Hz	$^{3}J_{9-10}$ 8.3 Hz		
											$^{4}J_{6-10}$ 1.8 Hz		
	^{13}C	100.8	183.7	120.9	140.7	127.1	110.0	147.8	149.3	115.4	122.8	55.1	
$Ga(CUR)_2^+$	^{1}H	6.02		6.76	7.77		7.24			6.84	7.14	3.92	
		s, 1H		d, 2H	d, 2H		d, 2H			d, 2H	dd, 2H		
				$^{3}J_{3-4}$ 15.6 Hz	$^{3}J_{3-4}$ 15.6 Hz		$^{4}J_{6-10}$ 1.4 Hz			$^{3}J_{9-10}$ 8.2 Hz	$^{3}J_{9-10}$ 8.2 Hz		
											$^{4}J_{6-10}$ 1.4 Hz		
	^{13}C	102.5	184.4	123.1	142.0	127.1	110.4	148.0	149.1	115.2	123.0	55.0	
bDHC	^{1}H	6.10		6.82	7.65 d, 2H		7.20		7.23	7.34	6.99	3.86	
		s, 1H		d, 2H	$^{3}J_{3-4}$ 15.9 Hz		d, 2H		m, 2H	t, 2H	m, 2H		
				$^{3}J_{3-4}$ 15.9 Hz			$^{4}J_{6-10}$ 1.8 Hz		$^{3}J_{8-9}$ 8.0 Hz	$^{3}J_{8-9}$ 8.0 Hz	$^{3}J_{8-9}$ 8.0 Hz		
									$^{4}J_{6-10}$ 1.8 Hz	$^{3}J_{9-10}$ 8.0 Hz	$^{4}J_{6-10}$ 1.8 Hz		
									$^{4}J_{8-10}$ 1.8 Hz		$^{4}J_{8-10}$ 1.8 Hz		
	^{13}C	101.1	183.2	124.2	140.5	136.6	112.4	160.1	115.6	126.4	120.5	54.9	
$Ga(bDHC)_2^+$	^{1}H	6.15		6.95	7.82		7.21		7.25	7.35	7.01	3.85	
		s, 1H		d, 2H	d, 2H		d, 2H		m, 2H	t, 2H	m, 2H		
				$^{3}J_{3-4}$ 15.6 Hz	$^{3}J_{3-4}$ 15.6 Hz		$^{4}J_{6-10}$ 1.7 Hz		$^{3}J_{8-9}$ 7.9 Hz	$^{3}J_{8-9}$ 7.9 Hz	$^{3}J_{8-9}$ 7.9 Hz		
									$^{4}J_{6-10}$ 1.7 Hz	$^{3}J_{9-10}$ 7.9 Hz	$^{4}J_{6-10}$ 1.7 Hz		
									$^{4}J_{8-10}$ 1.7 Hz		$^{4}J_{8-10}$ 1.7 Hz		
	^{13}C	103.6	184.7	126.4	142.3	136.7	113.1	160.2	116.5	126.5	121.0	55.0	
DAC	^{1}H	6.10		6.83	7.67		7.37			7.26	7.10	3.90	2.29
		s, 1H		d, 2H	d, 2H		d, 2H			d, 2H	dd, 2H		
				$^{3}J_{3-4}$ 15.8 Hz	$^{3}J_{3-4}$ 15.8 Hz		$^{4}J_{6-10}$ 1.5 Hz			$^{3}J_{9-10}$ 8.2 Hz	$^{3}J_{9-10}$ 8.2 Hz		
											$^{4}J_{6-10}$ 1.4 Hz		
	^{13}C	101.2	183.2	124.4	139.8	134.4	111.3	151.9	140.9	123.1	120.8	55.0	19.0
$Ga(DAC)_2^+$	^{1}H	6.15		6.95	7.82		7.10			7.37	7.27	3.88	2.29
		s, 1H		d, 2H	d, 2H		d, 2H			d, 2H	dd, 2H		
				$^{3}J_{3-4}$ 15.5 Hz	$^{3}J_{3-4}$ 15.5 Hz		$^{4}J_{6-10}$ 1.5 Hz			$^{3}J_{9-10}$ 8.1 Hz	$^{3}J_{9-10}$ 8.1 Hz		
											$^{4}J_{6-10}$ 1.5 Hz		
	^{13}C	103.1	184.7	126.8	141.4	134.4	111.6	151.6	141.0	123.1	121.0	54.8	18.8

[a]The splitting pattern, integrated area, and coupling constants are given below the ^{1}H chemical shift.

and 420 nm, the ratio of $\varepsilon(GaL_2^+)/\varepsilon(L)$ is much greater for CUR than it is for the other curcuminoids. This finding hints at a stronger interaction of $[Ga(CUR)_2]^+$ with BSA with respect to the other complexes. The $\varepsilon(GaL_2^+)/\varepsilon(L)$ values are reported in Supporting Information, Table 1S.

As shown in Figure 7, both ligands and metal complexes displayed broad emission peaks in the spectral region of 400–650 nm. Wavelengths of the emission maxima are reported in Supporting Information, Table 2S. In the same solvent system CUR and DAC did not show significant shifts of the emission maxima when their Ga^{3+} complexes were formed, while a weak red shift of the emission maximum was observed for bDHC ($\Delta\lambda(ML_2\text{-}L) \approx 10$ nm). Furthermore, the electronic effects of the substituents on the aromatic rings, and especially on their ability to form intramolecular and/or intermolecular hydrogen bonds, strongly influenced the fluorescence of free ligands. In fact, emission increased proportionally with the reduced ability of curcuminoids to form hydrogen bonds with the solvent (in the order bDHC < CUR < DAC), as previously observed for other CUR derivatives.[18]

Addition of metal ions commonly induces a dramatic quenching of the fluorescence emission.[19,20] Conversely, the addition of Ga^{3+} resulted in a nonquenching or slight quenching effect, playing the role of an almost inert and transparent linker between ligand molecules.[21] The quenching

dx.doi.org/10.1021/ic403113z | Inorg. Chem. 2014, 53, 4922–4933

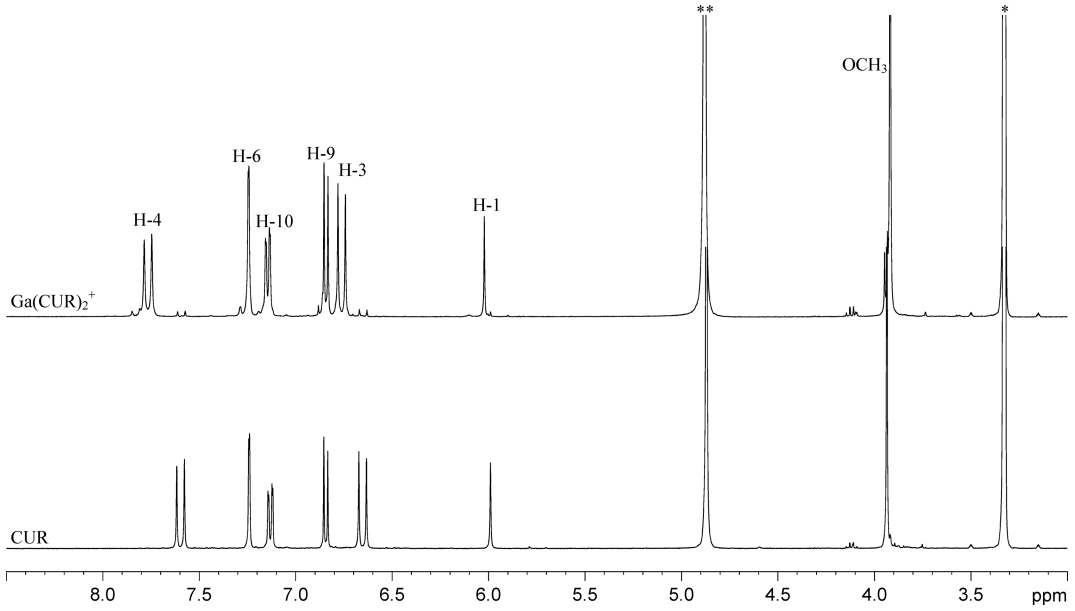

Figure 5. The ^{1}H NMR spectra of CUR and its 1:2 (Ga^{3+}/L) molar ratio complex in CD_3OD at 298 K with protons assignment (* residual CH_3OH signals, ** residual HOD signals).

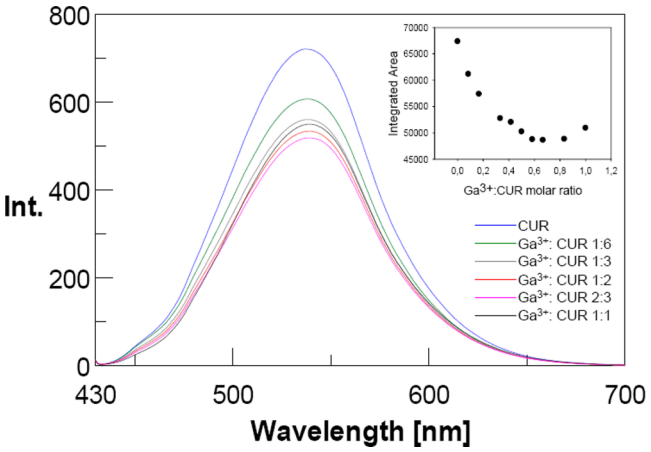

Figure 6. Emission spectra (λ_{ex} 420 nm) of CUR in MeOH (3 μM) with progressively added $Ga(NO_3)_3$ methanol solution (from top to bottom). (inset) The plot of emission peak integrated area vs Ga^{3+}/CUR molar ratio. All spectra were obtained at 298 K.

or increase in fluorescence emission due to metal complexation may be expressed as R_Φ, according to eq 2:

$$R_\Phi = \frac{\Phi_{F(ML)}}{\Phi_{F(L)}} = \frac{Area_{ML}}{Area_L} \times \frac{A_L}{A_{ML}} \times \frac{n_{ML}^2}{n_L^2} \quad \text{(eq 2)}$$

where Φ_F represents fluorescence quantum yield, Area stands for integrated emission peak area, A is absorbance at λ_{ex}, and n is the refraction index of medium. L stands for the free ligand, while ML represents the gallium complex $Ga(L)_2^+$. For the investigated curcuminoids, R_Φ (Figure 8) was only weakly affected by the medium, whereas substituents on the aromatic rings seem to be the driving force in affecting fluorescence emission. CUR and DAC behaved similarly; their fluorescence emission is quenched when gallium ion is added, up to the complete metal complex formation. They are characterized by $R_\Phi \approx 0.5$ in BSA. On the other hand, bDHC fluorescence emission was strongly increased in the presence of Ga^{3+}, as confirmed by R_Φ values close to 2, resulting in an opposite behavior with respect to the fluorescence trend for free ligands. These findings may suggest the key role of the substituents on aromatic rings in affecting the fluorescence of CUR derivatives. Actually, bDHC is characterized by only a little hindered substituent (the methoxy group meta to the aliphatic chain), which is able to act as a H-acceptor group both with the solvent and with BSA. Conversely, this interaction is prevented by intramolecular hydrogen bonds between H-donor phenolic group and H-acceptor oxygen of methoxy group in CUR and by the presence of a bulky acetyl group in DAC. Moreover, as

Table 3. Molar Extinction Coefficient ε [M^{-1} cm^{-1}] of All Ligands and Gallium Complexes

compound[a]	$\varepsilon_{(MeOH)}$[b]	$\varepsilon_{(W)}$[c]	$\varepsilon_{(PBS)}$[d]	$\varepsilon_{(BSA)}$[e]
		λ = 400 nm		
CUR	45 230	19 313	14 569	18 824
bDHC	35 541	17 362	16 581	22 131
DAC	33 251	19 147	17 587	23 133
$Ga(CUR)_2^+$	87 922	43 317	40 685	62 300
$Ga(bDHC)_2^+$	72 906	39 553	38 270	47 148
$Ga(DAC)_2^+$	68 629	41 527	37 678	51 537
		λ = 420 nm		
CUR	60 785	21 417	15 024	19 650
bDHC	23 349	15 098	14 839	18 569
DAC	24 969	14 278	13 750	18 796
$Ga(CUR)_2^+$	119 904	44 243	41 985	63 933
$Ga(bDHC)_2^+$	50 536	39 747	38 341	45 163
$Ga(DAC)_2^+$	58 932	33 850	31 159	44 348
		λ = 488 nm		
CUR	6788	3790	5200	9391
bDHC	1882	3680	4244	6583
DAC	296	1553	2061	5822
$Ga(CUR)_2^+$	26 633	14 870	18 207	38 022
$Ga(bDHC)_2^+$	7041	9787	9781	13 622
$Ga(DAC)_2^+$	2025	6393	5026	15 137

[a]Spectra were obtained at 298 K. [b]In MeOH. [c]In water (W). [d]In PBS buffered solution (PBS). [e]In the presence of BSA.

dx.doi.org/10.1021/ic403113z | Inorg. Chem. 2014, 53, 4922−4933

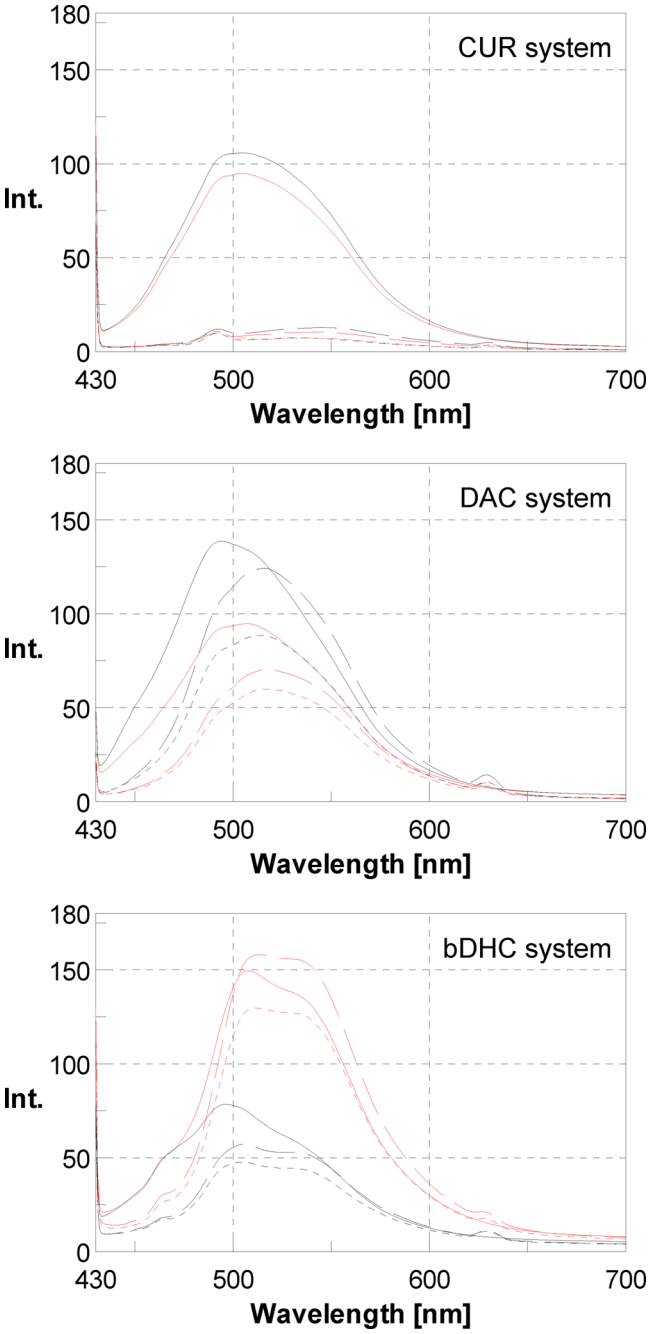

Figure 7. Emission spectra (λ_{ex} = 420 nm) of free ligands (CUR, DAC, and bDHC) (in black) and their Ga^{3+} complexes (in red) in different solvent systems: water (dashed line), pH 7.4 PBS (dotted line), and 5 mg/mL BSA solution in pH 7.4 PBS buffer (solid line). [L] = 6 μM, [Ga^{3+}] = 3 μM in pure water; [L] = 5.4 μM, [Ga^{3+}] = 2.7 μM in PBS buffered solution.

previously reported for another series of curcuminoids,[7] the electronic effects of the substituents influence ligand basicity, in the order bDHC > DAC > CUR. This finding may account for a stronger interaction of $Ga(bDHC)_2^+$ with BSA, which is negatively charged[22] at pH 7.4, and consequently for a higher rigidity of this BSA adduct with respect to that of the other curcuminoids.

2.5. Radiolabeling of Curcuminoids with Gallium-68. The synthesis path of curcuminoid complexes was adapted to short half-lived radionuclide chemistry, mainly considering the

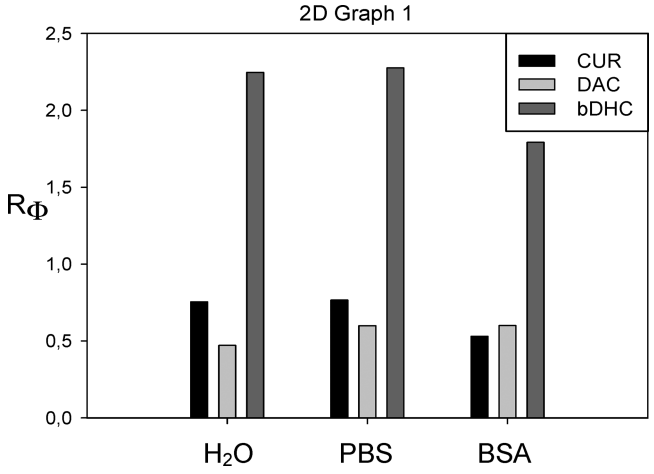

Figure 8. R_Φ for CUR (black), DAC (light gray), and bDHC (gray) in the three investigated media: H_2O pH ≈ 5; PBS pH = 7.4; and PBS + BSA (5 mg/mL) pH = 7.4. R_Φ are calculated at λ_{ex} = 420 nm.

high acidity and the aqueous eluting media of the $^{68}Ge/^{68}Ga$ generator (0.05 M HCl). A scheme of the synthetic procedures is shown in Figure 9. The complexation reaction of CUR and of

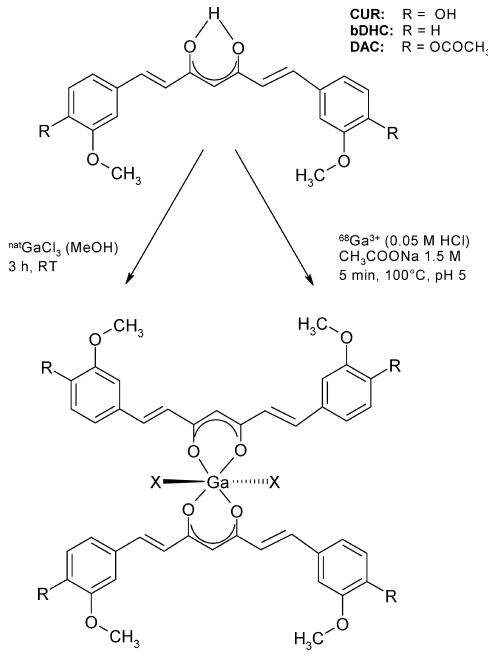

Figure 9. Synthetic path of the $^{nat/68}Ga$-curcuminoid complexes.

the two CUR derivatives with gallium-68 exhibited a strong pH dependence. For all the compounds, a radiochemical yield (RCY) greater than 95% could be obtained at pH 5, but it rapidly decreased for CUR and bDHC when the reactions were performed at pH 4 and pH 6, respectively. Conversely, DAC is able to label over a considerably larger pH range since the yield remained more than 90% and more than 60%. This behavior can be correlated to the higher DAC stability over pH with respect to the other curcuminoids, as reported by Basile et al.[23] The dependence of the RCY of the three curcuminoids as a function of the reaction pH is shown in Figure 10. Kinetics of the reactions was also studied as a function of temperature and time. For all the compounds, a RCY greater than 95% could be achieved already after 5 min under heating (373 K), while lower

dx.doi.org/10.1021/ic403113z | Inorg. Chem. 2014, 53, 4922−4933

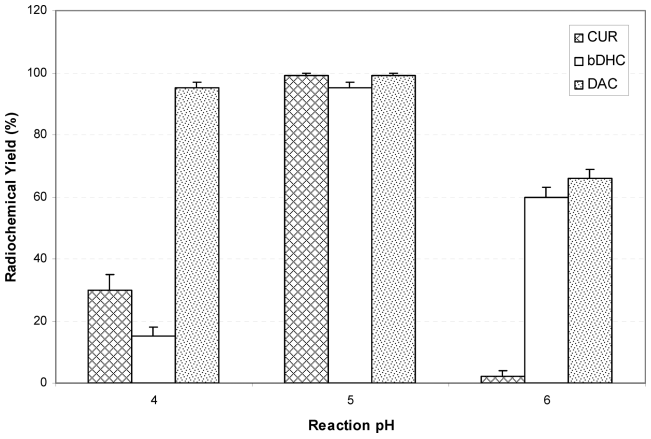

Figure 10. Radiochemical yield of the complexation reaction of the CUR derivatives (bDHC and DAC) and CUR itself when labeled with gallium-68 as a function of the reaction pH (60 nmol of precursor, 373 K, 5 min).

temperatures need longer time, which is generally not suitable for labeling with short half-lived radiometals such as gallium-68. As an example, the behavior of the reaction with CUR as a function of time and temperature is summarized in Figure 11.

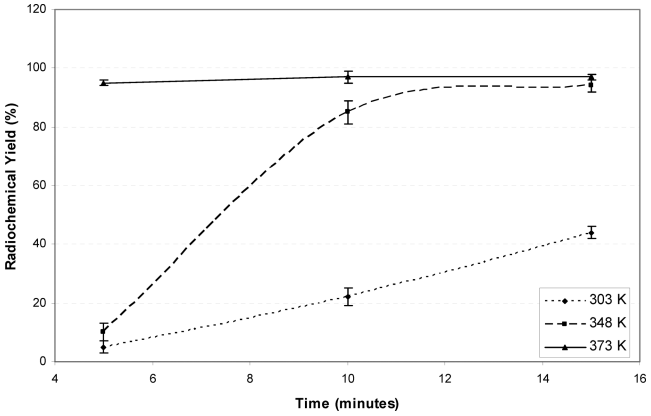

Figure 11. Radiochemical yield of the complexation reaction of CUR with gallium-68 ($n \geq 3$) as a function of temperature and time (pH = 5, 60 nmol of precursor).

bDHC and DAC exhibited comparable trends, but higher RCYs could be achieved also at lower temperatures, as reported in Supporting Information, Figure 5S. Afterward, the best reaction conditions (373 K, 5 min, pH 5), found in the first set of experiments, were applied for studying the dependence of the RCY on the precursor amount. The labeling reaction yield was >95% for all the precursors when ≥60 nmol of curcuminoids was used, but the formation of $^{68}Ga(CUR)_2^+$ and $^{68}Ga(bDHC)_2^+$ complexes appears little more favored than the formation of $^{68}Ga(DAC)_2^+$ complexes, as derived from the trend shown in Figure 12.

2.6. Quality Controls on the Gallium-68 Labeled Preparations. A satisfactory ultrahigh-performance liquid chromatography (UHPLC) separation could be achieved for $^{68}Ga(CUR)_2^+$ preparations, obtaining the following retention times: $^{68}Ga^{3+}$ = 1 min, ^{68}Ga-hydrolyzed products = 1.5 min, $^{68}Ga(CUR)_2^+$ = 4.0 min. Quality controls and stability studies of $^{68}Ga(bDHC)_2^+$ and $^{68}Ga(DAC)_2^+$ preparations were performed instead by radio-thin layer chromatography

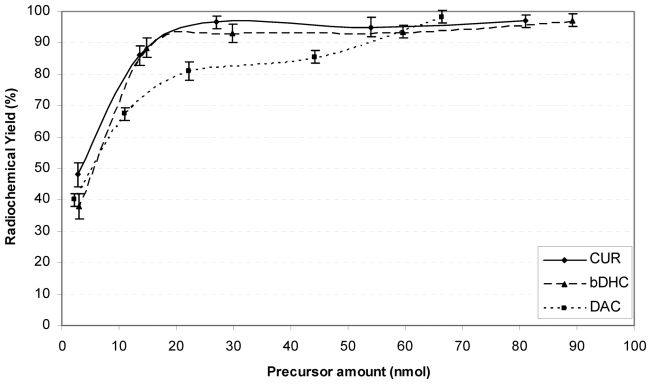

Figure 12. Radiochemical yield of the complexation reaction between the CUR derivatives (bDHC and DAC) and CUR itself with gallium-68 ($n \geq 3$) as a function of precursor amount (373 K, 5 min, pH = 5).

(TLC), obtaining the following R_f values: ^{68}Ga-curcuminoids = 0.0−0.2; ^{68}Ga-DTPA = 0.5 (DTPA = diethylenetriaminepentaacetic acid); free $^{68}Ga^{3+}$ and ^{68}Ga-hydrolyzed products = 0.9−1.0. When the best labeling conditions were used, the radiochemical purity (RCP) of all the ^{68}Ga-curcuminoid complexes was >95% so no further purification was performed. As a result, in the best labeling conditions (60 nmol), the maximum amount of free ligand in the final solutions was considered equal to the precursor amount added to the preparations.

2.7. Stability of ^{68}Ga-Curcuminoids Complexes, Transchelation, and Transmetalation Studies. All curcuminoid complexes showed high and comparable stability to transchelation and transmetalation when challenged with a 200 μM DTPA solution or with a 100 nM Fe^{3+}, Cu^{2+}, and Zn^{2+} solution. In all cases, the percentage of intact complex remained >95% over 120 min of incubation. When incubated with 0.9% NaCl solution or human serum, the stability of all ^{68}Ga-curcuminoids remained >90% over 120 min.

2.8. Affinity of $^{nat/68}$Ga-Curcuminoid Complexes for Aβ(1−40) Amyloid Synthetic Fibrils. Native CUR, and some fluorinated curcuminoids as well, has shown high binding affinity for β-amyloid plaques.[24] Moreover, ^{18}F-labeled or ^{99m}Tc-labeled CUR derivatives appeared suitable for in vivo imaging of AD.[25,5] Hence, as a first assessment of the biological application of the ^{68}Ga-curcuminoids complexes, the preservation of the affinity for β-amyloid fibrils in vitro was evaluated. When ^{68}Ga-curcuminoid complexes were incubated with synthetic β-amyloid fibrils, the radioactivity associated with the fibrils was 87 ± 4%, 90 ± 1%, and 48 ± 2% for $^{68}Ga(CUR)_2^+$, $^{68}Ga(DAC)_2^+$, and $^{68}Ga(bDHC)_2^+$, respectively, while, in the negative controls performed with free-$^{68}Ga^{3+}$, the measured activity was 0.02 ± 0.001%. The presence of curcuminoids and ^{nat}Ga-curcuminoid complexes associated with the fibrils was also qualitatively assessed by fluorescence microscopy, and the fluorescence intensity was compared to that emitted by untreated β-amyloid fibrils. The images clearly indicated a higher intensity of the treated samples with respect to the fibrils, confirming the affinity of all the compounds for the synthetic amyloid fibrils and, at the same time, excluding that the fluorescence was only due to phenomena of autoemission of the fibrils. Therefore, the ^{68}Ga-complexes appeared to maintain a high (CUR, DAC) or moderate (bDHC) affinity for synthetic β-amyloid fibrils. However, it is not guaranteed that the same affinity will be maintained also for

dx.doi.org/10.1021/ic403113z | Inorg. Chem. 2014, 53, 4922−4933

naturally occurring fibrils such as those expressed in Alzheimer's disease. The reduced affinity of $Ga(bDHC)_2^+$ could be mainly ascribed to the lower solubility and higher basicity of the ligands with respect to the other curcuminoids that might negatively influence the capability of the complex to interact with the synthetic fibrils. When ^{68}Ga-curcuminoids/amyloid fibrils samples were incubated with solutions containing a large molar excess of the corresponding curcuminoids, the radioactivity associated with the fibrils was sensibly lower, attesting to a displacement of 55 ± 2%, 44 ± 3%, and 16 ± 2% for $^{68}Ga\text{-}(CUR)_2^+$, $^{68}Ga(DAC)_2^+$, and $^{68}Ga(bDHC)_2^+$, respectively. Although these results appear encouraging, quantitative studies in vitro for determining the affinity constants and in vivo for evaluating the biodistribution of these radiotracers is needed for deriving final conclusions.

2.9. Uptake by Cancer Cells. Since it was previously shown that the uptake of CUR was significantly higher in tumor cells compared to normal cells,[23,26] as a second evaluation of the potential biological applications of the ^{68}Ga-curcuminoids complexes, the cellular fluorescence intensity associated with CUR, bDHC, and DAC was compared with the fluorescence intensity associated with the respective ^{nat}Ga-complexes when the compounds were internalized by A549 lung cancer cells. Cell cultures were incubated for 3 h with the varying compounds, fixed and analyzed by fluorescence microscopy, thus exploiting the intrinsic fluorescence of CUR and its derivatives as a qualitative marker of drug uptake. As shown in Figure 13, all the complexes showed a fluorescent intensity at least equivalent to the respective free curcuminoids. Many parameters must be considered before correlating fluorescence intensity and real cell uptake (i.e., different molar extinction coefficients, different intrinsic fluorescent emission, and different cell internalization mechanisms among the compounds); nevertheless, the qualitative observation clearly suggested that the Ga-curcuminoid complexes are internalized or bound by lung cancer cells. In particular, $Ga(DAC)_2^+$ fluorescence appeared more intense than that of the free DAC, while in the other compounds, the fluorescence appeared comparable. Moreover, fluorescence emitted by CUR appeared localized mainly in the nuclei, while fluorescence derived from DAC, bDHC, and gallium complexes appeared localized mainly in a perinuclear/cytoplasmic region. These different behaviors could be mainly ascribed (i) to the different hydrophobicity of the curcuminoids and complexes that probably alters the translocation mechanism across the cell membrane and (ii) to the presence or absence of intramolecular hydrogen bonds in the varying compounds that, analogously, influence the hydrophobicity and hence the localization inside the cells.

Additionally, to obtain a quantitative measurement of the fluorescence emitted by cells after the treatment with the different curcuminoids and complexes, flow cytometry analyses were performed. Results obtained are shown in Figure 14, where fluorescence of A549 treated cells is compared with the fluorescence of untreated cells in MeOH. Similarly to fluorescence microscopy, cells treated with $Ga(CUR)_2^+$ and $Ga(bDHC)_2^+$ showed a fluorescent intensity roughly equivalent to that of cells treated with the corresponding free ligands, while $Ga(DAC)_2^+$-treated cells showed higher fluorescence compared to the cells treated with DAC. In all cases, fluorescence associated with the treated cells was clearly superior to that of the untreated ones, ensuring that it originated from the compounds and not from autofluorescence phenomena.

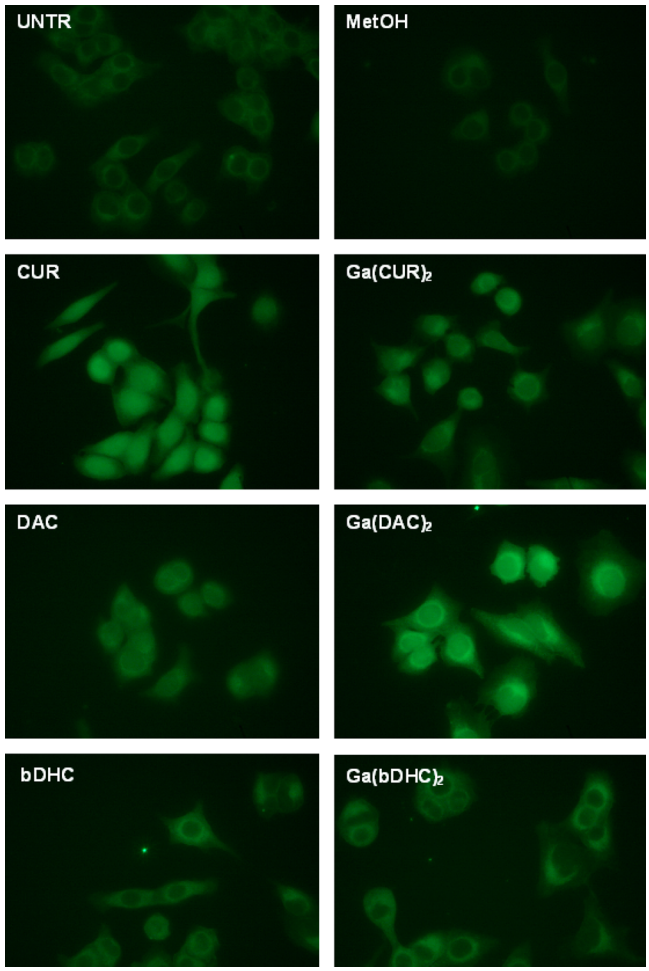

Figure 13. Images of the fluorescence associated with A549 untreated cells and A549 cells after treatment with free curcuminoids and Ga-curcuminoid complexes.

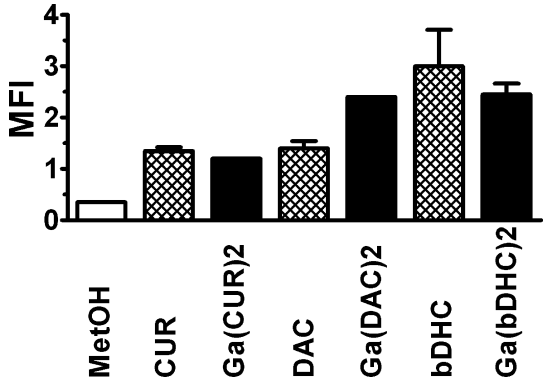

Figure 14. Fluorescence associated with untreated A549 cells or A549 cells treated with free curcuminoids and Ga-curcuminoid complexes. The mean fluorescence intensity (MFI) was quantified by flow cytofluorimetry.

Further evidence of the fact that the Ga-curcuminoid complexes were associated/internalized by the A549 cells was obtained when the experiments were performed by using the ^{68}Ga-labeled complexes. In this case, the final radioactivity associated with the cells was comparable for all the curcuminoids complexes and was between 0.25% and 0.28% of the initial injected radioactivity.

dx.doi.org/10.1021/ic403113z | Inorg. Chem. 2014, 53, 4922−4933

From these preliminary results, the ^{68}Ga-curcuminoids complexes show apparent potential as diagnostic tools for cancer detection in nuclear medicine applications, but further studies in vitro are needed for determining the quantitative uptake; above all, in vivo studies are needed for assessing the biodistribution of the compounds.

3. CONCLUSIONS

Complexes of CUR in the literature were introduced for a variety of biomedical applications such as antioxidants, antimicrobial, anticancer agents, and so forth. In this study, CUR and two curcuminoids (DAC and bDHC) were successfully labeled with gallium-68 to obtain potential positron emission tomography radiotracers and deeply characterized by means of mass spectrometry, NMR, UV−vis, and fluorescent spectroscopies. Ga-curcuminoid complexes, namely ^{68}Ga-$(CUR)_2^+$, ^{68}Ga$(DAC)_2^+$, and ^{68}Ga$(bDHC)_2^+$, were obtained in high radiochemical yield and purity. All the compounds showed high stability in saline, human serum, when challenged with DTPA or with Fe^{3+}, Zn^{2+}, and Cu^{2+} for transchelation or transmetalation studies. The results obtained when the biological behavior of these complexes was assessed are encouraging since ^{68}Ga$(CUR)_2^+$ and ^{68}Ga$(DAC)_2^+$ maintained a high affinity for synthetic β-amyloid fibrils, and all of the complexes showed a quite high uptake in lung cancer cells in vitro. Finally, the intrinsic fluorescent emission of the Ga-curcuminoid complexes introduces the possibility of synthesizing a mixed radioactive/fluorescent pharmacophore that can be exploited as a dual-mode imaging tool.

4. EXPERIMENTAL SECTION

4.1. Chemicals. Solvents and reagents for the curcuminoid synthesis, complexation, and characterization were purchased from Sigma-Aldrich, while Roswell Park Memorial Institute (RPMI) culture medium, fetal bovine serum, and PBS were purchased from EuroClone (Milan, Italy). Amyloid beta-protein (1−40) was purchased from Bachem (Bubendorf, Switzerland). 370 MBq itG ^{68}Ge/^{68}Ga generator was supplied by ITM (Garching, Germany), and metal-free hydrochloric acid (0.1 M) was purchased from Rotem (Leipzig, Germany). Human serum was obtained by healthy volunteers, and A549 lung cancer cell line samples were kindly provided by Dr. Sally Maramotti (Arcispedale Santa Maria Nuova-IRCCS, Reggio Emilia). When not differently stated, all commercial chemicals were used without further purification. When needed, Milli-Q water (resistivity 18.2 Mμ·cm) was used for preparing reagent solutions. Curcumin [1,7-bis(4-hydroxy-3-methoxyphenyl)-1,6-heptadiene-3,5-dione] (CUR), bis(dehydroxy)-curcumin [1,7-bis(3-methoxyphenyl)-1,6-heptadiene-3,5-dione] (bDHC), and diacetylcurcumin [1,7-bis(4-acetyl-3-methoxyphenyl)-1,6-heptadiene-3,5-dione] (DAC) were synthesized as previously reported by the authors.[7] Gallium(III) complexes were prepared by addition of a 5.7 mM $GaCl_3$ MeOH solution (2.85 μmol) to a 5.7 mM curcuminoid solution (5.0 μmol) in MeOH (CUR, DAC) or MeOH/dimethyl sulfoxide 3:1 (bDHC) and stirring the mixture for 3 h at room temperature (RT). The quantitative formation of GaL_2^+ species was confirmed by NMR data. All the complexes were characterized by NMR (^{1}H and ^{13}C) and matrix-assisted laser desorption ionization time-of-flight mass spectrometry (MALDI-TOF-MS). These data are summarized in Table 2 and Figure 5.

4.2. Computational Details. All calculations were performed with the Gaussian 03 package of programs,[27] and GaussView 03[28] was used as the plotting tool for data visualization. The computations were performed by DFT approaches, and the structures were fully optimized using hybrid-functional B3LYP applied to the 6-31G* basis set (B3LYP/6-31G*).

4.3. Instrumental Analysis. Ga-curcuminoid complexes were analyzed by MALDI-TOF-MS with a 4800 Plus MALDI TOF/TOF Analyzer (Applied Biosystem). Each spectrum represents accumulations of 1000 laser shots randomly selected on each spot. The reflectron mode was used. The ion source and flight tube pressure were less than 10^{-7} Torr. The MALDI mass spectrum of each gallium-curcuminoid complex in different Ga/L molar ratios (1:10, 1:5, 1:2, and 1:1) was recorded. Acquisition was performed both on the sample alone and using dithranol (DIT) as matrix, applying the conventional sample preparation method for MALDI-MS. 50 μL of Ga-complex methanol solution at the M/L molar ratios reported above ([L] ≈ 1 ppm) were diluted with 50 μL of H_2O, and then 1 μL was spotted on the sample holder alone or added, when dried, with 1 μL of DIT (10 mg/mL in CH_2Cl_2). The sample holder was then inserted in the ion source for analysis.

NMR spectra were recorded on a Bruker Avance AMX-400 spectrometer with a Broad Band 5 mm probe in inverse detection. Nominal frequencies were 100.13 MHz for ^{13}C, 122.026 MHz for ^{71}Ga, and 400.13 MHz for ^{1}H. For each sample 0.5 mL of millimolar solution was prepared in MeOD-d_4. Synthesis of Ga^{3+}/curcuminoid complex in MeOD-d_4 was obtained in situ by adding to millimolar ligand solution (0.5 mL) the proper addition of $Ga(NO_3)_3$ solution to reach the 1:2 metal-to-ligand molar ratio. Spectra were registered after few minutes from addition. Typical parameters were used for 2D correlation spectroscopy (COSY), NOESY, heteronuclear single quantum correlation (HSQC), and heteronuclear multiple-bond correlation (HMBC) experiments. 1D selective NOE experiments were applied using selective refocusing with a Gaussian-shaped pulse and a mixing time of 600 ms, implemented in the Bruker library sequence, namely, selnoegp.[29]

UV−vis absorption measurements were performed using a Jasco V-570 spectrophotometer in the range of 200−600 nm, while fluorescence experiments were carried out on a Jasco FP-6200 spectrofluorometer; emission spectra were obtained upon excitation within the lowest-energy absorption bands of the keto−enol isomer (λ_{ex} 400, 420, 450, and 488 nm). All measurements were performed at 298 K. Free ligands (L) and 1:2 gallium-to-ligand molar ratio systems were investigated in methanol, pure water, PBS, and in PBS with the addition of BSA (5 mg/mL). The curcuminoid concentration in each solvent system ([CUR] in MeOH = 3 μM; [bDHC] in MeOH = 3 μM; [DAC] in MeOH 4.5 μM; [L] = 6 μM in water, 5.4 μM in PBS solution, and in the presence of BSA) allowed a value of absorbance at λ_{max} (namely, 420 nm for CUR and 400 nm for bDHC and DAC) in the range of 0.1−0.2.

Radiochemical and chemical analyses were performed by ultrahigh-performance liquid chromatography (UHPLC) using an Acquity system with a binary solvent, BEH C-18 1.7 μm (2.1 × 150 mm) column, and autosampler manager modules (Waters, Milan, Italy). The instrument was equipped with an Acquity TUV detector (Waters, Milan, Italy) and a Herm LB 500 radiochemical detector (Berthold Technologies, Milan, Italy). Radiochemical purity was also assessed by TLC, using an AR 2000 Imaging Scanner device (Bioscan, Washington, DC, US). The pH of the samples was assessed by a pH 213 Microprocessor pH meter (Hanna Instrument, Milan, Italy). Activity measurements were performed with an Aktivimeter ISOMED 2000 dose calibrator (MED Nuklear-Medizintechnik, Dresden, Germany).

Fluorescence microscopy analyses were performed with a Nikon Eclipse 90i fluorescence microscope (equipped with a band-pass filter for acquiring the emission between 515 and 555 nm wavelength), and images were captured with NIS Elements software Nikon (Exposure: 1.5 s; Gain: 2.8×; Contrast: Medium) with a 100× oil immersion objective after exciting the samples at a 488 nm wavelength. Fluorescence associated with A549 cells after incubation with the compounds was evaluated at a 525 nm wavelength by flow cytometry using a Cytomics FC 500 system (Beckman Coulter, Milan, Italy) after exciting the samples at a 488 nm wavelength.

4.4. Radiolabeling of the Curcuminoids with Gallium-68. The ^{68}Ge/^{68}Ga generator was eluted with 4 mL of metal-free 0.05 M hydrochloric acid, and the curcuminoids were dissolved in EtOH (CUR) or acetonitrile (ACN) (DAC, bDHC) to obtain 1 mg/mL solutions. The reactions were initially performed by the addition of 60

dx.doi.org/10.1021/ic403113z | Inorg. Chem. 2014, 53, 4922−4933

nmol of curcuminoid to 350 μL (about 72 MBq) of the generator eluate followed by the addition of different amounts of a 1.5 M sodium acetate solution to study the best reaction conditions (pH from 4 to 6). Kinetics of the reaction was optimized by heating every sample to varying temperature (303, 348, 373 K) for varying times (5, 10, 15 min). After this optimization was accomplished, varying amounts of curcuminoids were added to 350 μL of generator eluate at a fixed pH, temperature, and time. Advancement of the reactions was assessed by radio-UHPLC (CUR) and radio-TLC (DAC, bDHC). Radiochemical yields were calculated considering the radiochemical purity obtained from UHPLC or TLC analyses. If not differently stated, all experiments were performed in triplicate and were conducted in 3 mL, flat bottom, glass vessels.

To identify the chromatographic peaks during the analyses and to identify the species formed during the transchelation experiments, free $^{68}Ga^{3+}$ (as chloroaquo complexes in solution), ^{68}Ga-hydrolyzed products solutions, and ^{68}Ga-DTPA complexes were obtained as described in references 30 and 31, respectively. Each ^{68}Ga-curcuminoid complex identity and stoichiometry was attested to by UHPLC coinjection of the corresponding ^{nat}Ga-complex, obtained as described before and analyzed by MALDI-TOF-MS.

4.5. Stability of ^{68}Ga-Curcuminoids Complexes, Transchelation, and Transmetalation Studies. For the stability, transchelation, and transmetalation studies, every ^{68}Ga-curcuminoid complex was synthesized by using 60 nmol of precursor at pH 5 and at 373 K for 15 min. Aliquots of ^{68}Ga-curcuminoid complex solutions (0.3 mL, approximately 20 MBq) were alternatively mixed to (i) 0.3 mL of a 0.9% NaCl, (ii) 0.3 mL of healthy human serum solution, (iii) 0.3 mL of a 200 μM DTPA solution, or (iv) 0.3 mL of a 100 nM Fe^{3+}, Cu^{2+}, or Zn^{2+} solution. The mixtures were incubated at 300 K and analyzed after 0, 10, 30, 60, and 120 min by means of UHPLC or radio-TLC analysis.

4.6. Quality Controls. Quality control on every radioactive preparation involving CUR was performed by UHPLC at a flow rate of 0.35 mL/min using ACN and a 0.1% v/v trifluoroacetic acid (TFA)/water solution as mobile phase with the following gradient: 0−2 min 22% ACN, 2−4 min 22−80% ACN, 6−7 min 80−100% ACN. The wavelength of the UV detector was set to 300 nm, and the column temperature was fixed to 303 K. Alternatively, for the DAC and bDHC preparations, radio-TLC analyses were performed with RP-18F plates (Merck, Whitehouse Station, NJ, USA) as stationary phase and a 97% 0.1 M sodium citrate/3% 1 M HCl solution as mobile phase.

4.7. Aβ(1−40) Amyloid Fibrils Preparation. Amyloid fibrils were prepared according to methods previously published.[32,33] Briefly, 0.5 mg of β-amyloid protein was dissolved in 1 mL of filtered PBS, pH 7.4, and magnetically stirred at 760 rpm for 3 d at RT, resulting in a visibly cloudy solution. The mixture was centrifuged at 25 830 *g* for 15 min to separate Aβ fibrils from soluble, not-aggregated Aβ proteins. The supernatant was removed, and the Aβ fibrils pellet was washed twice with PBS before being suspended in 1 mL of filtered PBS. The fibrils formation was confirmed by Congo Red binding assay.

4.8. Affinity of ^{68}Ga-Curcuminoids Complexes for Aβ(1−40) Amyloid Synthetic Fibrils. The amyloid fibrils solution was stirred to homogenize the suspension, and aliquots of 70 μL (35 μg) were incubated at 300 K for 10 min with (i) 500 μL (ca. 74 MBq) of the ^{68}Ge/^{68}Ga generator elution containing free-$^{68}Ga^{3+}$ (as a negative controls) or 500 μL (ca. 20 MBq) of ^{68}Ga-curcuminoids complexes, respectively, and (ii) 500 μL of a 50 μM solution of curcuminoids and ^{nat}Ga-curcuminoid complexes. The mixtures were centrifuged at 25 830 g for 15 min, the supernatants were removed, and the fibril pellets were washed twice with filtered PBS before being measured in the dose calibrator (i) or visualized by fluorescence microscopy (ii). Displacement tests were performed by adding 500 μL of a 10 μM solution of curcuminoids to the respective ^{68}Ga-complexes/amyloid fibrils samples obtained as described above. The mixtures were homogenized by stirring and incubated at 300 K for 10 min. Subsequently, the samples were centrifuged at 25 830 *g* for 15 min and washed twice with PBS before being measured again in the dose calibrator.

4.9. Cell Cultures and Uptake Studies. For cellular fluorescence studies, 2.5 mM stock solutions of free curcuminoids and ^{nat}Ga-curcuminoid complexes were prepared in MeOH as described in Section 4.1 (Chemicals). The complete formation of GaL_2^+ species was confirmed by NMR experiments. A549 lung cancer cells were seeded in RPMI supplemented with 10% fetal bovine serum (FBS) at 20 000 cells/well in 4-well chamber slides (Lab-Tek II, EuroClone) and allowed to adhere overnight in a 5% CO_2 incubator at 300 K. The medium was removed, and cells were incubated for 3 h in 500 μL of RPMI + 10% FBS with free curcuminoid or ^{nat}Ga-curcuminoid complexes at 10 μM or 5 μM concentration, respectively. Cells were then washed twice with PBS, fixed with 4% paraformaldehyde for 10 min at room temperature, washed again with PBS, air-dried, and covered with a glycerol-based mounting medium to decrease fading of fluorescence. Fluorescence associated with the cells incubated with the compounds was evaluated by fluorescence microscopy and flow cytometry and was compared with the fluorescence of untreated A549 cells.

For cellular radioactive uptake studies, A549 cancer cells were prepared as described above but were subsequently incubated at 300 K with 500 μL (ca. 72 MBq) of ^{68}Ga-curcuminoid complex solution. Internalization was stopped at 30 min by removing the medium and washing the cells twice with ice-cold PBS. Finally, the cells were detached with 2 mL of trypsin/ethylenediaminetetraacetic acid 0.25% solution and centrifuged to separate the supernatant from the cells pellet. The radioactivity associated with the pellets was measured in the dose calibrator.

■ ASSOCIATED CONTENT

Supporting Information

Listing of spectroscopic data (Table 1S, Table 2S, Figure 3S, and Figure 4S), NMR data (Figure 1S and Figure 2S), and radiochemical data (Figure 5S). This material is available free of charge via the Internet at http://pubs.acs.org.

■ AUTHOR INFORMATION

Corresponding Author

*E-mail: asti.mattia@asmn.re.it.

Notes

The authors declare no competing financial interest.

■ ACKNOWLEDGMENTS

E.F. is grateful to the Centro Interdipartimentale Grandi Strumenti—CIGS of the University of Modena and Reggio Emilia, especially to Dr. Diego Pinetti and Dr. Maria Cecilia Rossi for technical assistance and useful suggestions. E.F. and M.S. thank the Fondazione Cassa di Risparmio di Modena for supplying mass spectrometers. The authors want to thank Prof. Rois Benassi for his support and expertise in theoretical calculations. The authors are also thankful to the Arcispedale Santa Maria Nuova-IRCSS (Reggio Emilia, Italy) and ITG (Garching, Germany) for supporting the project PHYTORAD.

■ REFERENCES

(1) Kovacevic, Z.; Kalinowski, S. D.; Lovejoy, B. D.; Yu, Y.; Rahmanto, S. Y.; Sharpe, C. P.; Bernhardt, V. P.; Richardson, R. *Curr. Top. Med. Chem.* **2011**, *11*, 483−499.

(2) Zandi, K.; Ramedani, E.; Mohammadi, K.; Tajbakhsh, S.; Deilami, I.; Rastian, Z.; Fouladvand, M.; Yousefi, F.; Farshadpour, F. *Nat. Prod. Commun.* **2010**, *5*, 1935−1938.

(3) Cheng, K. K.; Yeung, C. F.; Ho, S. W.; Chow, S. F.; Chow, A. H. L.; Baum, L. *AAPS J.* **2013**, *15*, 324−336.

(4) Ferrari, E.; Asti, M.; Benassi, R.; Pignedoli, F.; Saladini, M. *Dalton Trans.* **2013**, *42*, 5304−5313.

(5) Sagnou, M.; Benaki, D.; Triantis, C.; Tsotakos, T.; Psycharis, V.; Raptopoulou, C. P.; Pirmettis, I.; Papadopoulos, M.; Pelecanou, M. *Inorg. Chem.* **2011**, *50*, 1295−1303.
(6) Roesch, F.; Riss, P. J. *Curr. Top. Med. Chem.* **2010**, *10*, 1633−1668.
(7) Ferrari, E.; Pignedoli, F.; Imbriano, C.; Marverti, G.; Basile, V.; Venturi, E.; Saladini, M. *J. Med. Chem.* **2011**, *54*, 8066−8077.
(8) Cai, X. Z.; Huang, W. Y.; Qiao, Y.; Du, S. Y.; Chen, Y.; Chen, D.; Yu, S.; Che, R. C.; Liu, N.; Jiang, Y. *Phytomedicine* **2013**, *20*, 495−505.
(9) Ostrowski, W.; Śniecikowska, L.; Hoffmann, M.; Fransi, R. *J. Spectrosc.* **2013**, *2103*, 1−8.
(10) Sagnou, M.; Benaki, D.; Triantis, C.; Tsotakos, T.; Psycharis, V.; Raptopoulou, C. P.; Pirmettis, I.; Papadopoulos, M.; Pelecanou, M. *Inorg. Chem.* **2011**, *50*, 1295−1303.
(11) Benassi, R.; Ferrari, E.; Lazzari, S.; Spagnolo, F.; Saladini, M. *J. Mol. Struct.* **2008**, *892*, 168−176.
(12) Mague, J. T.; Alworth, W. L.; Payton, F. L. *Acta Crystallogr., Sect. C: Cryst. Struct. Commun.* **2004**, *C60*, o608−o610.
(13) Xu, M.; Dou, X.; Bu, Y.; Zhang, Y. *Chem. Phys. Lett.* **2012**, *537*, 101−106.
(14) Kubícék, V.; Havlíčková, J.; Kotek, J.; Tircsó, G.; Hermann, P.; Tóth, E.; Lukeš, I. *Inorg. Chem.* **2010**, *49*, 1060−10969.
(15) Chaves, S.; Mendonça, A. C.; Marques, S. M.; Prata, M. I.; Santos, A.; Martins, A. F.; Geraldes, C. F.G.C.; Santos, M. A. *J. Inorg. Biochem.* **2011**, *105*, 31−38.
(16) Kumar, A.; Li, L.; Chaturvedi, A.; Brzostowski, J.; Chittigori, J.; Pierce, S.; Samuelson, L. A.; Sandman, D.; Kumar, J. *Appl. Phys. Lett.* **2012**, *100*, 203701.
(17) Kunwar, A.; Barik, A.; Pandey, R.; Priyadarsini, K. I. *Biochim. Biophys. Acta* **2006**, *1760*, 1513−1520.
(18) Caselli, M.; Ferrari, E.; Imbriano, C.; Pignedoli, F.; Saladini, M.; Ponterini, G. *J. Photochem. Photobiol., A* **2010**, *210*, 115−124.
(19) Kim, S.-H.; Gwon, S.-Y.; Burkinshaw, S. M.; Son, Y.-A. *Spectrochim. Acta, Part A* **2010**, *76*, 384−387.
(20) Leung, M. H. M.; Pham, D.-T.; Lincoln, S. F.; Kee, T. W. *Phys. Chem. Chem. Phys.* **2012**, *14*, 13580−13587.
(21) Fages, F.; Leroy, S.; Soujanya, T.; Sohna Sohna, J.-E. *Pure Appl. Chem.* **2001**, *73*, 411−414.
(22) Salgin, S.; Salgin, U.; Bahadir, S. *Int. J. Electrochem. Sci.* **2012**, *7*, 12404−12414.
(23) Basile, V.; Ferrari, E.; Lazzari, S.; Belluti, S.; Pignedoli, F.; Imbriano, C. *Biochem. Pharmacol.* **2009**, *78*, 1305−1315.
(24) Lee, I.; Yang, J.; Lee, J. H.; Choe, Y. S. *Bioorg. Med. Chem. Lett.* **2011**, *21*, 5765−5769.
(25) Ryu, E. K.; Choe, Y. S.; Lee, K. H.; Choi, Y.; Kim, B. T. *J. Med. Chem.* **2006**, *49*, 6111−6119.
(26) Kunwar, A.; Barik, A.; Mishra, B.; Rathinasamy, K.; Pandey, R.; Priyadarsini, K. I. *Biochim. Biophys. Acta* **2008**, *1780*, 673−679.
(27) Frisch, M. J.; Trucks, G. W.; Schlegel, H. B. et al. *GAUSSIAN 03,* Revision D.01; Gaussian, Inc.: Wallingford, CT, 2004.
(28) Dennington, II R.; Keyth, T.; Millam, J.; Eppinnett, K.; Hovell, W. L.; Gilliand, R. *Gaussview,* Version 3.0; Semichem, Inc.: Shawnee Mission, KS, 2003.
(29) Stott, K.; Stonehouse, J.; Keeler, J.; Hwang, T. L.; Shaka, A. J. *J. Am. Chem. Soc.* **1995**, *117*, 4199−4200.
(30) Asti, M.; Iori, M.; Erba, P. A.; et al. *Nucl. Med. Commun.* **2012**, *33*, 1179−1187.
(31) Asti, M.; Iori, M.; Capponi, P. C.; Atti, G.; Rubagotti, S.; Martin, R.; Brennauer, A.; Müller, M.; Bergmann, R.; Erba, P. A.; Versari, A. *Nucl. Med. Biol.* **2014**, *41*, 24−35.
(32) Klunk, W. E.; Jacop, R. F.; Mason, R. P. *Anal. Biochem.* **1999**, *266*, 66−76.
(33) Agdeppa, E.; Kepe, V.; Liu, J.; Torres, S. F.; Satyamurthy, N.; Petric, A.; Cole, G. M.; Small, G. W.; Huang, S. C.; Barrio, J. R. *J. Neurosci.* **2001**, *21*, 1−5.